


Article

Identifying Original and Restoration Materials through Spectroscopic Analyses on Saturnino Gatti Mural Paintings: How Far a Noninvasive Approach Can Go

Letizia Bonizzoni ^{1,*}, Simone Caglio ², Anna Galli ², Chiara Germinario ³, Francesco Izzo ^{4,5}
and Donata Magrini ⁶

¹ Dipartimento di Fisica Aldo Pontremoli, Università degli Studi di Milano, Via Celoria 16, 20133 Milano, Italy

² Dipartimento di Scienza dei Materiali, Università degli Studi di Milano-Bicocca, 20125 Milano, Italy; simone.caglio@unimib.it (S.C.); anna.galli@unimib.it (A.G.)

³ Department of Science and Technology, University of Sannio, Via de Sanctis, 82100 Benevento, Italy; chiara.germinario@unisannio.it

⁴ Department of Earth Sciences, Environment and Resources, Federico II University, Via Cinthia, 80126 Naples, Italy; francesco.izzo4@unina.it

⁵ CRACS—Center for Research on Archaeometry and Conservation Science, 80126 Naples, Italy

⁶ ISPC-CNR, Istituto di Scienze del Patrimonio Culturale, CNR, Area della Ricerca di Firenze, Via Madonna del Piano, 10, 50019 Sesto Fiorentino, Italy; donata.magrini@cnr.it

* Correspondence: letizia.bonizzoni@unimi.it

Abstract: This paper presents the results obtained for the mural paintings (XV century CE) in the church of San Panfilo in Villagrande di Tornimparte (AQ, Italy) by means of noninvasive spectroscopic techniques; this research is a part of the project on the Saturnino Gatti pictorial cycle, promoted and coordinated by the AIAR (the Italian Archaeometry Association). Digital optical microscopy (OM), X-ray fluorescence spectroscopy (XRF), fiber optics reflectance spectroscopy in the UV–Vis–NIR range (FORS), Fourier transform infrared spectroscopy in the external reflection mode (ER-FTIR), and Raman spectroscopy were performed on the points selected based on the image analysis results and the few available records on previous intervention, with the aim of characterizing both the original and restoration organic and inorganic materials. The synergic application of complementary techniques allowed us to obtain a complete picture of the palette and the main alteration products and organic substances (of rather ubiquitous lipid materials and less widespread resin and proteinaceous materials in specific points). The identification of modern compounds permitted the individuation of restoration areas; this was confirmed by the comparison with multiband imaging results, as in the case of specific green and blue pigments, strictly related to the presence of high signals of zinc. This analytical protocol left only very few ambiguities and allowed to minimizing the number of samples taken to clarifying, by sample laboratory analyses, the few doubts still open.

Keywords: mural painting; Saturnino Gatti; Italian Archaeometry Association; XRF; FORS; ER-FTIR; Raman spectroscopy; pigments; binders



Citation: Bonizzoni, L.; Caglio, S.; Galli, A.; Germinario, C.; Izzo, F.; Magrini, D. Identifying Original and Restoration Materials through Spectroscopic Analyses on Saturnino Gatti Mural Paintings: How Far a Noninvasive Approach Can Go. *Appl. Sci.* **2023**, *13*, 6638. <https://doi.org/10.3390/app13116638>

Academic Editor: Giuseppe

Lacidogna

Received: 14 April 2023

Revised: 26 May 2023

Accepted: 28 May 2023

Published: 30 May 2023



Copyright: © 2023 by the authors. Licensee MDPI, Basel, Switzerland. This article is an open access article distributed under the terms and conditions of the Creative Commons Attribution (CC BY) license (<https://creativecommons.org/licenses/by/4.0/>).

1. Introduction

This paper contributes to the Special Issue, Results of the II National Research Project of AIAR: Archaeometric Study of the Frescoes by Saturnino Gatti and Workshop at the Church of San Panfilo in Tornimparte (AQ, Italy), in which the scientific results of the II National Research Project, conducted by members of the Italian Association of Archaeometry (AIAR), are discussed and collected. For in-depth details on the project's aims, see the introduction of the Special Issue [1].

It is worth explaining that Tornimparte, its hamlet Villagrande, and the entire L'Aquila region suffered a major earthquake in 1703. We do not have a precise record of the damage suffered by the buildings, but it is quite relevant to the fact that the present houses are all

post-1700, and the churches are all designed in the Baroque style. Indeed, San Panfilo in Villagrande is a remarkable exception; however, we can speculate it was damaged by the disaster, too. This same region was affected by another great earthquake in 1915 and then again in 2009, which devastated the whole area.

The ultimate goal of the project is to support the foreseen restoration interventions following the last earthquake through the complete study of the conservation status and the characterization of the original materials, the superimposed ones, and the degradation phenomena affecting the wall paintings. The project involved several Italian groups working on cultural heritage materials: for each aspect of the research, a selected team of researchers from the participant groups was involved. The analyses performed within the project comprise micro-climatic monitoring, multispectral imaging and photogrammetric surveying, degradation mapping, and thermography investigations, alongside the in situ and laboratory material characterizations.

One of the first steps of the study's project of the pictorial cycle, attributed to Saturnino Gatti at the church of San Panfilo in Villagrande di Tornimparte, is the one presented in this paper. Indeed, immediately after the imaging analyses (used as exploratory techniques for the choice of the region of interest for our study and as the first approach to distinguish between the original and restored areas), noninvasive spectroscopic techniques were applied with the aim of characterizing both original and restoration organic and inorganic paint materials. Namely, digital optical microscopy (OM), X-ray fluorescence spectroscopy (XRF), fiber optics reflectance spectroscopy in the UV–Vis–NIR range (FORS), Fourier transform infrared spectroscopy in the external reflection mode (ER-FTIR), and Raman spectroscopy were used. Each one of these techniques has its own place in the cultural heritage field, and they are often used together in order to overcome specific limits. The synergic application of analytical techniques, exploiting different radiation frequency ranges, indeed allows for obtaining complementary information for a complete picture of the palette [2–5], main alteration products [6–9] and organic substances [10–14]. Despite the poor conservation state of the decorative materials and the presence of several retouched and restored areas, the analytical approach adopted here provided very informative results, not only for the identification of original materials but also for the identification of modern compounds, allowing the individuation of restored areas that can be confirmed and highlighted by results obtained by imaging results [15]. In the present contribution, preliminary outputs are illustrated, and allowed to suggest a few areas, then selected for additional sampling and laboratory analyses.

2. Materials and Methods

Tornimparte Church, the parish church located in Villagrande, a hamlet of Tornimparte, is dedicated to Panfilo di Sulmona and dates back to around the year 1000. It still retains the original architectural forms, although profound renovations were made following the 1461 and the 1703 L'Aquila earthquakes, being a building located in an area with a high seismic risk. The most important intervention, however, took place in 1495, when Saturnino Gatti, a local young artist that can be fully considered an exponent of the Renaissance, painted in the apsis of the church a sequence of frescoes. The artistic work in Tornimparte Church has miraculously survived until today and is essentially the only testimony of Saturnino Gatti's mural paintings, while several of his easel paintings and sculptures still survive.

The frescoes underwent a number of restoration interventions: the first one we know about dates back to 1929, and even if there are no written documents describing it, the existence of still pictures allows us to understand that restorers worked mainly on the faces of several characters [16]. It is worth noting that these same areas are nowadays very damaged. A second known intervention was then made in 1951, and the last one in 1972, following a fire caused by a short circuit in 1958. Starting from this problematic condition, the evaluation of material characterization comes to light as a necessary step before further restoration works following the 2009 earthquake and needs to be in cooperation with the local government authorities for cultural heritage (Segretariato regionale del ministero per i

Beni e le Attività Culturali e per il Turismo per l'Abruzzo, and Soprintendenza Archeologia, Belle Arti e Paesaggio per la Città dell'Aquila e i comuni del Cratere).

2.1. Selected Areas

The mural paintings of San Panfilo Church were created around 1495 by Saturnino Gatti. In the middle of the vault is the representation of Paradise: the Eternal Father is the central figure surrounded by Angels and the Blessed. In the arch above the main altar, the Prophets who predicted the coming of the Redeemer are depicted, while on the side, Archangel Gabriel is shown in the act of announcing the birth of the Son of God to the Virgin. Around the apsis, in five separate panels, the moments of the Redemption are reproduced: the capture of Jesus and the kiss of Judas in the Garden of Olives, the scourging, the crucifixion, the Deposition of Christ, and the Resurrection of the Savior.

The measuring points were selected on three of the above-described panels of the lower part of the apsis and on the blue background on the vault. For a more detailed description of the mural paintings, please refer to [1]. The panels considered for the noninvasive spectroscopic investigations were the Garden of Olives (panel A in the following), the Deposition of Christ (panel E in the following), and the Resurrection (panel D in the following). The selection of measuring points was made with the supervision and support of the Superintendent Inspectors of the Italian Ministry of Culture and the restorers, taking into account the geometrical limitations for the movements of the instruments. The selected regions are representative of the original painting layers and of the various restoration interventions, either documented or supposed; the panels and the investigated points (about 60 for the entire cycle) are reported in Figure 1. Moreover, thanks to the close coordination of the project, this noninvasive approach was performed after and on the basis of the results obtained by imaging techniques [17]; in particular, visible images under ultraviolet light and infrared reflectography were used to serve as exploratory techniques, allowing to recognize regions of interest for the study and to distinguish between the original and restored sections in an artwork.

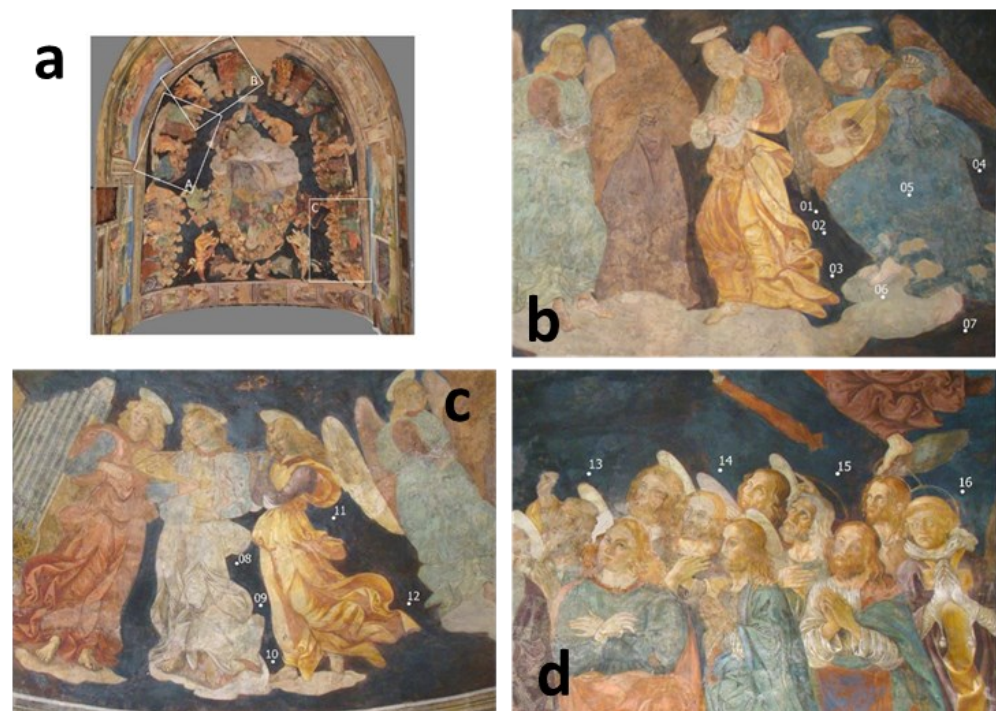


Figure 1. Cont.



Figure 1. Pictures of the analyzed scenes and investigated points: (a) panels on the vault; (b–d) analyzed points on the vault; (e) the Resurrection, details of investigated points; (f) Garden of Olives, investigated points; (g,h) the Resurrection, details and investigated points.

2.2. Analytical Techniques

As already stated, several complementary noninvasive techniques were applied, as detailed in the following paragraphs. For obvious reasons, the exploitation of portable instrumentations and techniques is highly preferable: the ultimate goal of the present campaign was to acquire as much information as possible about both original and restoring organic and inorganic materials in order to minimize the number of samples required for laboratory investigations.

2.2.1. Optical Digital Microscopy (OM) in Visible Light

Magnified images were obtained by a Dino-Lite portable digital microscope, with a CCD sensor of 5 Mpx for each point of analysis. The 50× and 200× magnifications were considered. For a correct focus on the surface, the microscope head was gently placed on the wall.

2.2.2. Fiber Optics Reflectance Spectroscopy in the UV–Vis–NIR Range (FORS)

Fiber optics reflectance spectroscopy in the UV–Vis–NIR range was performed using a FORS spectrometer (StellarNet BlueWave) working in the 400–1000 nm spectral range, with a resolution of 0.5 nm. The light source was a tungsten halogen lamp (2800 K, 200 W/m² power). The instrument allows the measurements in different geometry configurations and through different configurations of fiber optics. Due to the rough and opaque surface of the wall painting, to maximize the signal to be acquired, a 0/0 geometry (perpendicular to the wall surface and gently applied to the investigated areas) was chosen, exploiting a bifurcated fiber optic, which allows bringing the light to the sample and collecting the response signal from the same probe. To reduce the signal-to-noise ratio, an integration time of 500 milliseconds was used with the average over three scans.

2.2.3. Raman Spectroscopy

Raman spectra were acquired by means of an i-Raman Plus BW Tec in the fiber optics configuration; the fiber optics head, mounted in a plastic holder, was gently placed on the wall. The mounted laser had a wavelength of 785 nm with 320 mW of maximum power; the spectral range was 200–3000 cm⁻¹ with a resolution lower than 5 cm⁻¹. The laser power used was 8%, with a 10 s integration time and 3 accumulations for all the colors except the red ones, for which the power was 10% with a 10 s integration time and 5 accumulations.

2.2.4. Fourier Transform Infrared Spectroscopy

Infrared spectra were obtained via Fourier transform infrared spectroscopy (FTIR) on panels A, D, and E by using a Bruker Alpha portable FTIR spectrometer with an external reflectance (ER) module and equipped with a ROCKSOLID™ interferometer and a ZnSe/KBr beam splitter with a DTGS detector (room temperature). Circular areas of about 3 mm in diameter were analyzed by gently leaning the ER module on the wall for non-destructive analyses. The spectra were collected in the spectral range between 7500 and 400 cm⁻¹, with a resolution of 4 cm⁻¹, and a number of scans, variable from 64 to 192 (1–3 min). Opus 7.2 software was used for data acquisition and processing, treated by smoothing and log transformation ($A' = \log(1/R)$) [18].

2.2.5. X-ray Fluorescence Spectroscopy

Two different spectrometers were used for the XRF in situ analyses: one for the paintings on the walls of the apsis, and the other was a handheld model, which allowed working on the scaffolding for the vault.

The elementary analysis of the apsis walls was performed using a portable XRF Assing LITHOS 3000 spectrometer equipped with a Mo anode X-ray tube and a Peltier-cooled Si-PIN detector. The radiation is quasi-monochromatic at the energy of Mo K α energy by means of a Zr transmission filter; the X-ray tube mounts a 4 mm diameter collimator so that the irradiated area on the sample is about 25 mm². Data were collected using 25 kV high voltage and 0.3 mA tube current, with a 100 s acquisition time. The distance between the head of the device and the wall was about 10 mm.

The XRF analyses on the vault were instead performed using a Tracer III SD Bruker portable device equipped with a rhodium X-ray tube, a palladium anticathode, and a solid-state silicon detector energy dispersion system. The set-up was as follows: 40 keV and 12 μ A for 60 s; the instrument head, covered in soft plastic, was gently applied on the vault. The measuring area was an elliptical spot of 4 mm \times 7 mm. For data visualization and fitting, ARTAX software was used.

For both spectrometers, we based our considerations on the raw spectra fitting: we assigned each characteristic energy to the related chemical element and performed the relative intensity evaluation to acquire information about the chemical composition of the materials. From a methodological point of view, a comparison between the results obtained by two different commercial portable XRF spectrometers mounting X-ray tubes with different anode materials allows us to obtain the most from this technique. Indeed, experi-

ence suggests that spectrometers should be selected according to the specific requirements and type of analysis to perform, always keeping in mind the difficulty of also working on hard-to-access surfaces, such as the Tormiparte vault frescoes for which scaffolds were required [19].

3. Results and Discussion

The goal of the research was to provide as much information as possible by exploiting a noninvasive approach. It is well known that studying a mural painting is challenging for many reasons, the most important of which is the contemporary presence of plaster, pigments, degradation products, pollution, and restorations. Analyses virtually carry a huge amount of information, which is difficult to disentangle, as it is not trivial to clearly link an element or a compound to the corresponding material.

The in situ spectroscopic analyses have to be considered a necessary but insufficient condition for a complete characterization of the pictorial materials and techniques applied. They certainly have the advantage of helping in the mapping of pigment and binder presence. In addition, the joint use of the various spectroscopic techniques partially compensates for the intrinsic impossibility of uniquely identifying the present stratigraphy provided by the analyses performed on the micro-samples.

We thus performed the already mentioned analytical point-wise spectroscopic investigations and then compared the results with imaging investigations [17]. We thus inferred the type of materials (pigments and binders) and were able to distinguish between the original and restored areas. The association of the selected techniques makes it possible to overcome the limitations of each one and to detect all classes of pigments, binders, and alteration products. By using these results, areas for the samplings were then chosen to remove all remaining doubts.

3.1. Plaster

Spectra, acquired via ER-FTIR, detected the ubiquitous presence of calcium carbonate, the principal constituent of the wall paintings' support, featured by the undistorted $\nu_1 + \nu_3$ combination band of the $(\text{CO}_3)^{2-}$ group at ca. 2510 cm^{-1} (with a shoulder at ca. 2590 cm^{-1}), and the *Reststrahlen* and derivative effects at ca. 1410 cm^{-1} (with an asymmetric stretching band of CO_3), 873 cm^{-1} (with an "out-of-plane" bending vibration of the $(\text{CO}_3)^{2-}$ group), and 713 cm^{-1} (with an "in-plane" bending vibration of the $(\text{CO}_3)^{2-}$ group) [20]. Calcium and calcium carbonate in white areas and several color backgrounds were also detected, respectively, by XRF and Raman spectroscopy, as expected.

3.2. Pigments

The investigated areas were chosen together with the art historians and conservators examining the results of previously performed imaging analyses—both to have a complete picture of the original and added materials and to answer specific questions. In general, typical pigments of mural paintings were detected. Indeed, yellow and brownish hues were obtained by iron oxides and/or hydroxides, as well as red pigments, which constituted mostly of iron oxides. Only in a few cases were the red details executed by using vermilion, as, for instance, the darker vests seen in the A and E panels [1]. This pigment is easily recognized based on Raman spectra and from the presence of mercury in the XRF ones. In the left box, in Figure 2, the digital optical microscope image of a vest painted with vermilion in panel A is reported.

Flesh tones were obtained by mixing a calcium-based white pigment (see Section 3.2.2 for white characterization) with iron oxides and vermilion traces. In the restored areas, highlighted by the presence of high zinc signals in the XRF spectra and confirmed by imaging investigations [17], lead white was also detected based on the presence of high lead signals in the XRF spectra. The digital optical microscope image of a restored flesh tone in panel A is reported in the right box in Figure 2.

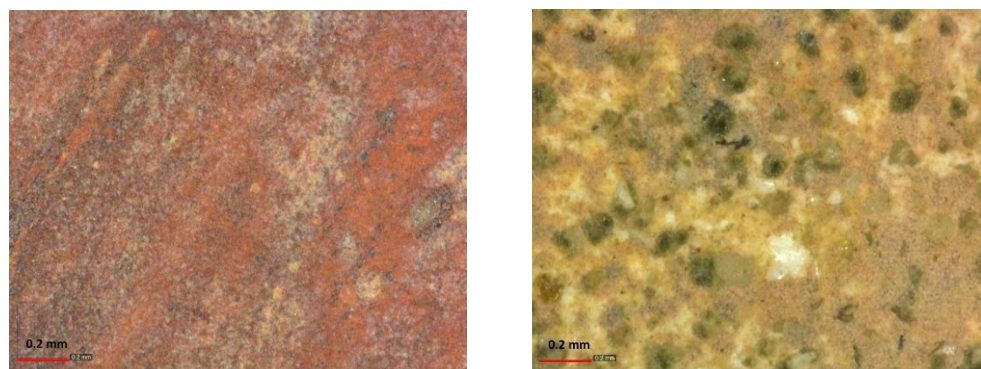


Figure 2. Digital optical microscope images: on the (left), panel A, dark red vest (ochre with vermilion); on the (right), panel A, flesh tone, restored area (ochres, lead white, and zinc white). Red scale bars correspond to 0.2 mm.

In the following sections, a deeper overview of the most interesting cases is provided. All the results are summarized in Table 1.

Table 1. Summary table of the pigment detected in the different investigated areas on panels A, D, and E.

Panel	Color	Pigments
Panel A, E	Green	Green earth with small quantities of a copper-based pigment
Panel A	Green	Green earth with zinc white with small quantities of chromium-based pigment
Panel A	Green	Green earth, zinc, and lead white, chromium-based pigment with small quantities of copper-based pigment
Panel E	Green	Green earth and other iron oxides
Panel A	Green	Copper-based pigment with lead white
Panel D	Green	Copper-based pigment, green earth, and zinc white
Panel E	Green	Copper-based pigment with green earth and zinc white
Panel A, D, E	Flesh tones	Iron oxides
Panel A	Flesh tones	Iron oxides with zinc and lead white
Panel A, E	Blue	Azurite
Panel A	Blue	Ultramarine with zinc and lead white
Panel D	Blue	Ultramarine with zinc white
Panel A	Blue	Prussian blue with zinc white
Panel A, D	Red	Iron oxides
Panel A, E	Red	Iron oxides with small quantities of vermilion
Panel E	Red	Vermillion
Panel A, D, E	Yellow	Yellow ochre
Panel D	Yellow	Yellow ochre and zinc white
Panel E	Yellow	Yellow ochre with small quantities of vermilion
Panel E	Brown	Iron oxides
Panel A, D, E	White	Calcite
Panel A	White	Calcite with small quantities of zinc white
Panel D	Black	Carbon or bone black

3.2.1. Green

At least two different past restorations are evident on the bases of the detected green pigments, where one was characterized by the use of a copper-based pigment and the other by a chromium-based green. Indeed, copper-based green and green earth were detected, either coupled in the same measured point or separated in different points (see Table 1 for details). This could possibly be linked to various restoration phases and can be related to imaging mapping [17]. For instance, in panel D, both copper-based green and green earth (this last supposed was to be the original material for greens) were detected together with high zinc signals in the XRF spectra, indicating a modern intervention, while in one detail on panel A, only copper-based green was found together with high signals of zinc,

indicating this pigment was surely used for restoration intervention. On the other hand, in the restored green areas of panel A, characterized by a high zinc presence, significant chromium signals were detected through XRF analysis. From the in situ noninvasive investigations, the green points left several open questions; for this reason, the green areas were chosen for sampling and laboratory analyses [21].

3.2.2. White

In all the investigated white areas, the analytical techniques applied indicate the presence of calcite, detected both as a calcium presence by XRF and as calcium carbonate by Raman spectroscopy. It is worth stressing that lead white was never detected in the white areas of the analyzed panels; however, it was sometimes detected (see Table 1) in the restored areas of the flesh tones (see Figure 2 right) coupled with the presence of zinc and thus related to modern restorations. Indeed, the presence of zinc white was mapped by UV fluorescence [17] as it exhibits a well-visible lemon-yellow fluorescence. The obtained images indicate a massive use of this pigment for retouching painting.

In the white shades, and in particular, in the highlights, the spectral evidence of proteinaceous materials was unveiled by ER-FTIR (Figure 3). Proteins were recognized by the stair-step pattern of the diagnostic absorption bands (Figure 3a) due to the stretching vibration of the C=O bond in the carbonyl group at ca. 1635 cm^{-1} (amide I), affected by the derivative distortion in external reflection, and the C-N stretching and N-H bending vibrations at ca. 1530 cm^{-1} (amide II). Moreover, they show the asymmetric stretching vibrations of methyl $\text{CH}_3\text{-CH}_2$ groups, respectively, at ca. 2980 , 2930 , and 2870 cm^{-1} [22,23].

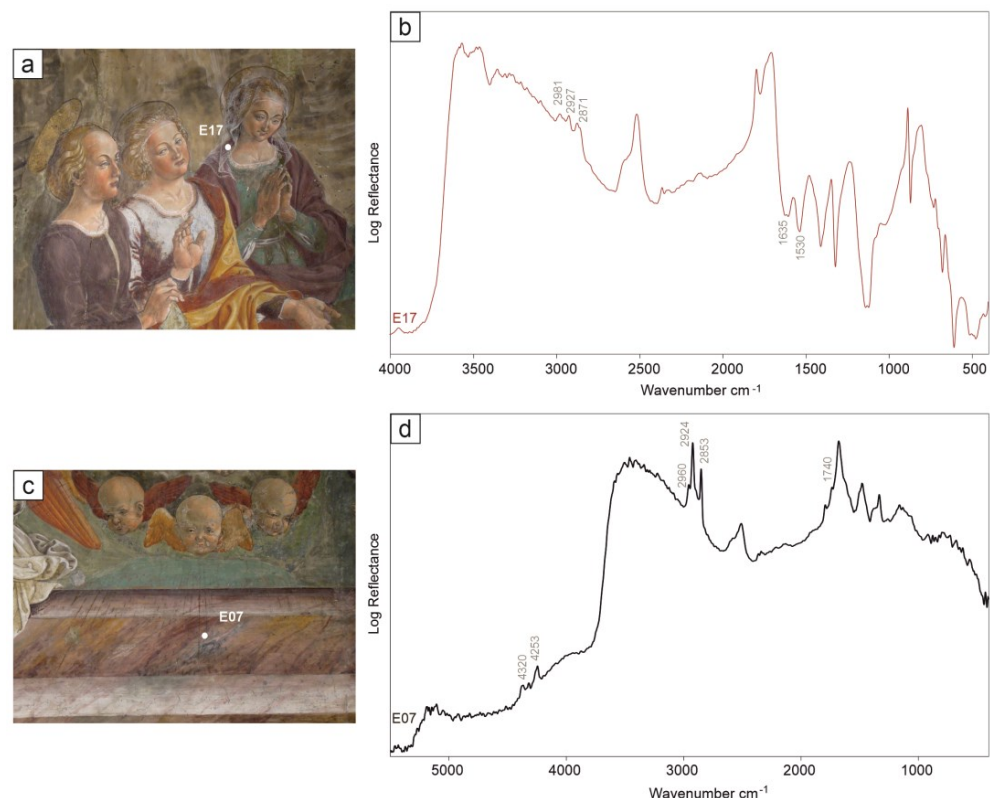


Figure 3. Infrared spectra, acquired at different points of panel E, reveal the use of proteinaceous materials for the highlights (a,b) and lipids for the gildings (c,d).

3.2.3. Blue

The combination of XRF, FORS, and Raman spectroscopy allowed the detection of several blue pigments related to the original and restoration areas pertaining to various interventions, according to the imaging analysis results [17]. On the panels, both azurite

and ultramarine were, in fact, detected in different areas, as highlighted by the combined use of the spectroscopic techniques and reported in Table 1. In particular, XRF can detect high copper contents in azurite, while FORS can clearly distinguish the two different materials. It is interesting to note that, both in panel A and in panel D, the presence of ultramarine is related to a high presence of zinc, as indicated by the XRF spectra. It is worth noting that azurite was mapped using the UV fluorescence images [17], thanks to the binder, as this pigment was usually applied using the “secco” technique [24,25]. On panels A and E, the typical infrared bands of azurite, at ca. 2592, 2557, and 2510 cm^{-1} ($\nu_1 + \nu_3$ combination band of $(\text{CO}_3)^{2-}$), along with the strong doublet at ca. 4380 and 4244 cm^{-1} (combination $\nu + \delta$ (OH) and overtone $3\nu_3$), were detected by ER-FTIR (Figure 4) [26]. In these areas, the XRF (high copper presence) and FORS spectroscopy indicated the use of this specific blue pigment. For blue pigments, as well as for green ones, a second restoration phase was highlighted by the use of Prussian blue. In fact, on panel A, the presence of the peak related to the carbon–nitrogen bond at ca. 2088 cm^{-1} in the ER-FTIR spectra suggested the use of Prussian blue (Figure 4) [27,28]. In this same area, the higher iron presence, along with the zinc signals in the XRF spectra, upholds a Prussian blue presence and confirms that it pertains to a modern restoration.

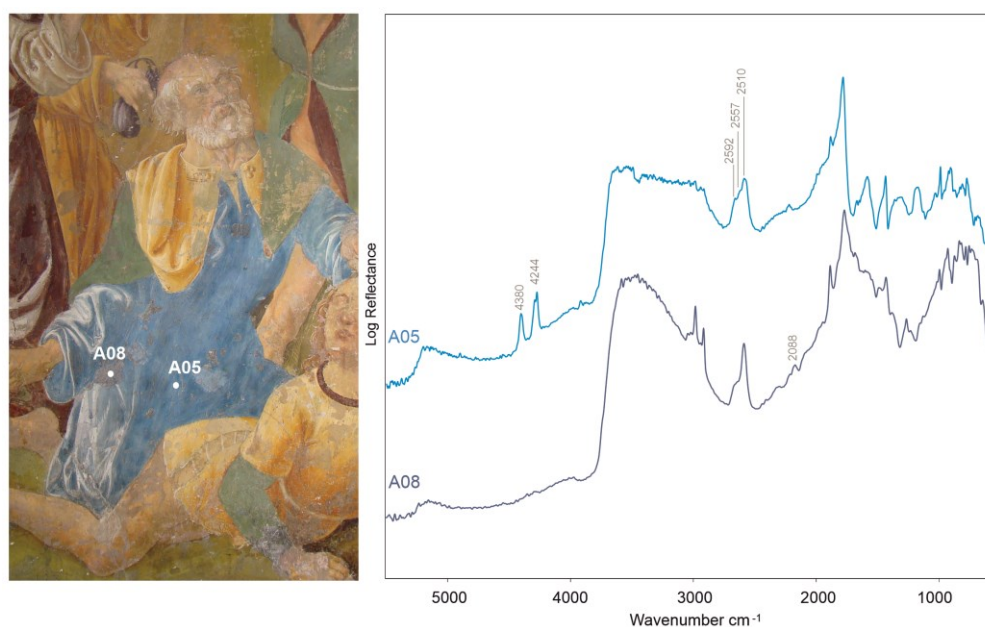


Figure 4. ER-FTIR spectra, acquired on a figure with the blue clothing on panel A, reveal the spectral evidence of azurite in the original area (A05) and Prussian blue in the restored part (A08).

Regarding the vault, instead, only XRF analyses were carried out, with the aim of investigating the composition of the blue background. However, due to problems relating to the height of the scaffold and the instrument placement, it was only possible to reach limited portions located in the lower part of the vault, while the top surfaces were not subjected to analysis. In all the spectra analyzed, as expected, high counts relating to calcium were observed. These are correlated to the Ca-rich matrix of the plaster. The calcium signals are always associated with those of strontium. Exceptions are the points analyzed in a single region of the vault (points V_08–V_12) in which the Sr signals are not detected; this could indicate that the calcium carbonate in that area was applied during restoration and shows a different geochemical signature. The XRF spectra also show intense counts relating to iron. The presence of this element, ubiquitously detected in the XRF spectra of all the areas of the vault analyzed, can be justified by the presence of a level of red preparation for the blue application, traditionally made with morellone [29]—an orange iron oxide and black carbon mixture applied on a calcite substratum. Copper signals are also always present, even if with very low intensities. These data allow us to hypothesize the presence

of residual original azurite, which was subsequently integrated with modern materials. Regarding the identification of the blue pigment used in the repainting, a hypothesis can be formulated regarding the use of a mixture of Prussian blue and zinc white, the latter highlighted by the UVF images showing the lemon-yellow luminescence characteristic of the pigment [17], as already verified in the apsis panels. Indeed, as aforementioned, the presence of the Prussian blue pigment was confirmed by the ER-FTIR and XRF spectral results and by the analyses on cross-sections of the retouched blue backgrounds present in different areas of the pictorial cycle [30].

A further assumption that can be formulated for the points where there are no characteristic elements linked to a precise blue pigment (e.g., copper or cobalt) is the presence of a level of morellone, which could justify the intense signals of iron, with a superimposed layer made with ultramarine and lead white, applied to integrate the original azurite. Additionally, in this case, the hypothesis is partially confirmed by the results of the sampling and by the subsequent analytical investigations on the cross-sections, which highlight the presence of this mixture in some portions of the bottom of the vault. It is worth noting that, as previously stated, ultramarine was detected in some of the restored areas (individuated by the presence of high Zn signals in XRF spectra) of the apsis panels, for instance, in the blue vests in panel D.

3.3. Gildings

The gildings displayed a presence of gold X-ray characteristic lines, L_{α} and L_{β} , in the XRF spectra, respectively, at 9.71 keV and 11.44 keV, and also in those areas where they are no longer visible to the naked eye. Some of these areas, if observed by a digital microscope (see Figure 5), show the presence of residual islands of gildings.

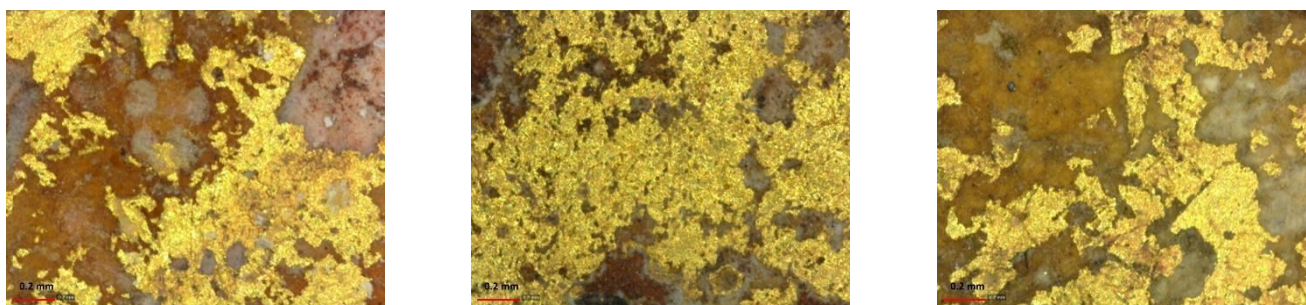


Figure 5. Digital optical microscope images for residual gildings: from the left, panel A, panel D, and panel E. Red scale bars correspond to 0.2 mm.

On the gold gildings, the ER-FTIR revealed the use of lipidic material (i.e., oil), likely used to adhere the gold leaf to the surface. On the spectra acquired on all analyzed panels, sharp and intense signals with a derivative shape relative to $\nu(\text{CH}_2/\text{CH}_3)$ stretching appear at ca. 2930 and 2860 cm^{-1} , along with a weaker shoulder at ca. 2960 cm^{-1} , as well as the derivative band at ca. 1750 cm^{-1} due to the carbonyl asymmetric stretching band [14]. Moreover, in the near-infrared region, the peculiar doublet was detected due to the combination of methylenic C–H stretching and bending at ca. 4345 and 4255 cm^{-1} (Figure 3d) [31]. As highlighted by the multiband imaging investigations [17] in specific areas, the presence of organic material allowed us to map the original presence of the gildings, which were also on some dresses and veils. Indeed, all these areas are characterized by a yellow–orange fluorescence in the UVF (ultraviolet fluorescence photography) images [17] due to the presence of organic material and, namely, the lipidic fraction of the so-called missione used to make the gold adhere. The missione is the preparation (and sticking) layer of the gildings, made using linseed oil and small quantities of pigments. This type of mapping allowed us to recognize the former presence of gildings in several other areas, such as in the rays that leave the angels in the Resurrection scene (panel D).

3.4. Organic Materials

The ER-FTIR spectroscopy proved particularly effective in unveiling the types of organic materials occurring on the wall paintings examined. Spectral features suggested, in fact, the rather ubiquitous presence of lipid materials (oils and/or waxes) along with less widespread resins.

In addition to the gildings, traces of oils were detected in most of the spectra acquired on panels A, E, and D, highlighted by the bands at ca. 4345, 4255, 2960, 2930, 2860, and 1750 cm^{-1} (Figure 6).

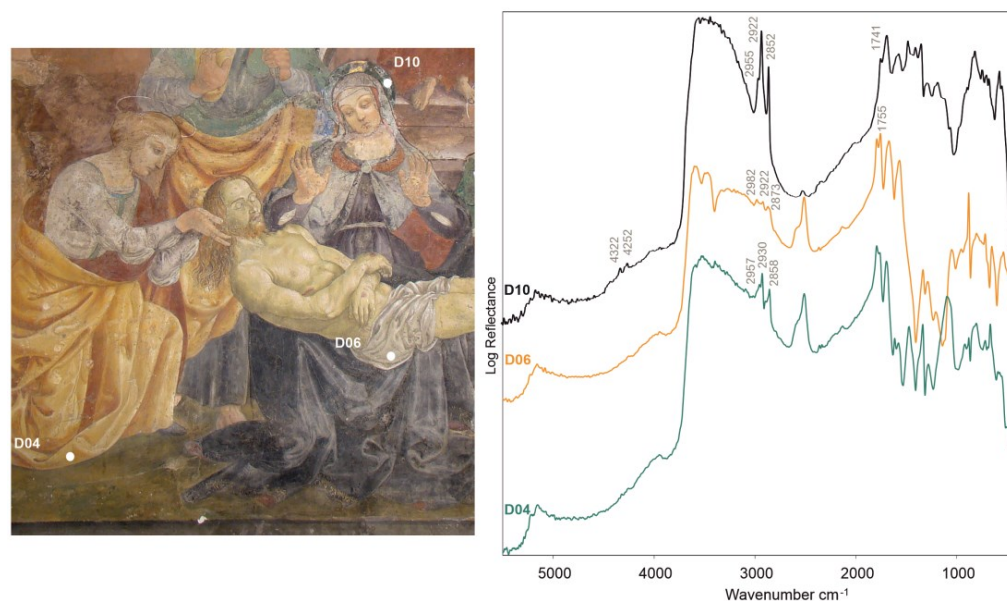


Figure 6. Detail of panel D, where oil (D10), resin (D06), and wax (D04) were detected.

Occasionally, instead, the spectral evidence of waxes and resins was observed. The waxes were easily distinguished by diagnostic CH_2 derivative-like stretching doublets at ca. at 2935 and 2858 cm^{-1} , with a weaker band near 2955 cm^{-1} (for the CH_3 stretching vibration, see Figure 6). The derivative effect at ca. 1740 cm^{-1} ($\text{C}=\text{O}$ stretching vibration) was only occasionally observed as a very weak band. Where it lacks, the presence of paraffin could be hypothesized. Resins, instead, are featured by three broader, medium-weak signals at ca. 2980, 2950, and 2850 cm^{-1} , although the most diagnostic band is visible at ca. 1750–1740 cm^{-1} , related to the $\text{C}=\text{O}$ stretching vibrations [22,23,32].

3.5. Alteration Products

The ER-FTIR also revealed the presence of specific alteration products affecting the wall paintings due to the alteration of the Ca-carbonate substrate and organic materials.

Most spectra from panels A, D, and E, in fact, showed the spectral evidence of calcium sulfate, featured by the broad bands at ca. 2230 ($2\nu_3 \text{SO}_4$; $\nu_2 + \nu_L \text{H}_2\text{O}$) and 2140 cm^{-1} ($\nu_1 + \nu_3 \text{SO}_4$) and peaks at ca. 1150 cm^{-1} (ν_3 antisymmetric SO_4 stretching vibration modes), 670, and 600 cm^{-1} (ν_4 antisymmetric SO_4 bending vibration modes), along with the O-H stretching bands between 3600 and 3400 cm^{-1} (Figure 7a) [20].

Calcium sulfate could have several origins, as ion sulfates can be present in the form of impurities in the plaster, or calcium sulfate can arise from the soil; sulfate species are dissolved in soil water and, for capillary action, migrate and crystallize on wall surfaces [33]. An alternative hypothesis linked to the high presence of retouched areas is that calcium sulfate comes from the pigments used by restorers, as most of the time, calcium sulfate was added to the rated pigment. Indeed, sub-efflorescence and efflorescence, with consequent detachment and disintegration, were observed on the restoration mortars near the windows of panels A and C and along the lower part of the apsidal conch [34]. It is also worth

noting that calcium sulfate was also detected in the samples from the Saturnino Gatti cycle through micro-stratigraphic analyses of thin sections [35] and the characterization of sampled soluble salts [36].

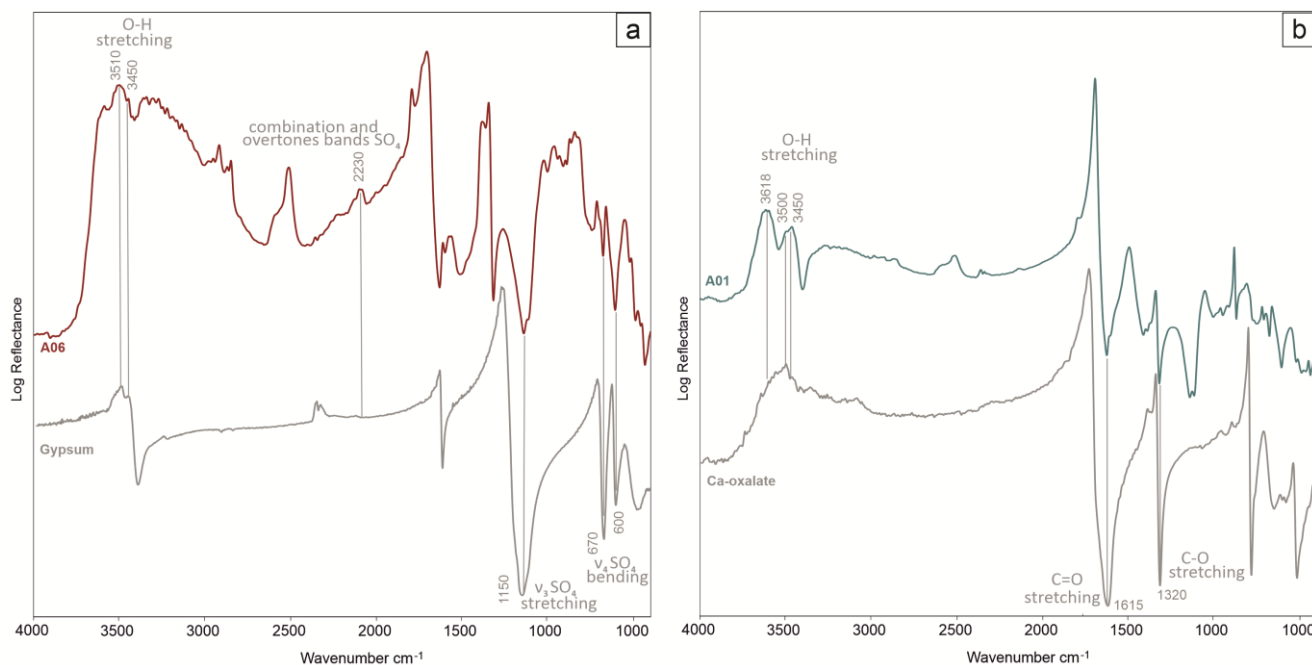


Figure 7. ER-FTIR spectra acquired on panel A show the spectral evidence of Ca-sulfates (a) and Ca-oxalates (b). Reference spectra [22] were also reported for comparison.

Moreover, in most spectra, the characteristic bands of calcium oxalate at ca. 1615 cm^{-1} (C=O vibration) and 1320 cm^{-1} (C-O vibration) were observed (Figure 7b) [22].

4. Conclusions

This paper presents one of the research activities in the frame of the study project of the pictorial cycle attributed to Saturnino Gatti at the church of San Panfilo in Villagrande di Tornimparte. The analytical campaign was promoted and coordinated by the AIAR (Italian Archaeometry Association) and established in cooperation with the Italian Ministry of Culture prior to the restoration works that became strictly necessary after the 2009 great earthquake in the region. In this context, we have presented the results obtained using in situ noninvasive analyses performed after, and guided by, the imaging techniques with the aim of characterizing the original and superimposed materials and, thus, allowing minimization of the sampling areas for further laboratory investigations.

The optimized analytical approach proposed, based on noninvasive diagnostics, proved to be powerful enough to characterize the present materials, ranging from the original pictorial layers to repainting and retouching, and to identify the techniques employed for the realizations of the wall paintings. The combination of elemental analysis with molecular characterization, provided by X-ray fluorescence and UV-vis spectroscopies, respectively, allows for the in situ noninvasive acquisition of a remarkable amount of information about the paint materials used by Saturnino Gatti. His palette comprises pigments, either used pure or in a mixture, to create different hues and are all compatible with the coeval pictorial technique. For the flesh tones, the artist used a mixture of calcium-based white with ochres/earths and amounts of vermilion. The presence of lead white has been, instead, highlighted in the retouched areas. Azurite was identified as the original pigment for the blue hues, while restorations occurred, probably at different times while using ultramarine or Prussian blue. Green earth, copper-based green, and chromium-based green were identified in different points or mixtures and probably pertained to the different

interventions in the artwork. For the red hues, Saturnino Gatti painted mainly using iron oxides; in a few cases, these were mixed or in superimposition with vermilion. For the yellow and brown tones, the original areas revealed iron hydroxides.

The noninvasive approach suggests the use of a gilding technique with a golden leaf adhered to a red bolus preparation in areas where it is no longer visible to the naked eye.

Moreover, in addition to the original palette, the analytical protocol identified modern paint materials, such as Prussian blue, zinc white, copper, and chromium-based greens, used for numerous retouching. The repainted areas analyzed are probably attributable to several conservation interventions carried out in different periods.

In conclusion, a strong synergy with the imaging techniques survey performed on the same pictorial cycle, allowed an implementation on the quality of the punctual analyses results, demonstrating how a well-designed noninvasive campaign permits to drastically reduce a sampling, necessary to complete the information on the materials and the artist's technique.

Author Contributions: Investigation, L.B., S.C., A.G., C.G., F.I. and D.M.; Data Curation, L.B., S.C., A.G., C.G., F.I. and D.M.; Visualization: L.B., C.G. and D.M.; Writing—Original Draft Preparation, L.B., C.G. and D.M.; Writing—Review and Editing, L.B., S.C., A.G., C.G., F.I. and D.M.; Supervision, A.G. All authors have read and agreed to the published version of the manuscript.

Funding: This work was performed in the framework of the Project Tornimparte—“Archeometric investigation of the pictorial cycle of Saturnino Gatti in Tornimparte (AQ, Italy)”, sponsored in 2021 by the Italian Association of Archeometry, AIAR (www.associazionear.com (accessed on 27 May 2023)).

Data Availability Statement: The data presented in this study are available on request from the Italian Association of Archeometry, AIAR (www.associazionear.com (accessed on 27 May 2023)).

Acknowledgments: The authors would like to thank the Proloco Tornimparte Association and the mayor of the municipality of Tornimparte for the availability and support shown during the diagnostic campaign.

Conflicts of Interest: The authors declare no conflict of interest.

References

1. Galli, A.; Alberghina, M.F.; Re, A.; Magrini, D.; Grifa, C.; Ponterio, R.C.; La Russa, M.F. Special Issue: Results of the II National Research project of AIAR: Archaeometric study of the frescoes by Saturnino Gatti and workshop at the church of San Panfilo in Tornimparte (AQ, Italy). *Appl. Sci.* **2023**. *to be submitted*.
2. Idjouadiene, L.; Mostefaoui, T.A.; Naitbouda, A.; Djermoune, H.; Mechehed, D.E.; Gargano, M.; Bonizzoni, L. First Applications of Non-Invasive Techniques on Algerian Heritage Manuscripts: The LMUHUB ULAHBIB Ancient Manuscript Collection from Kabylia Region (Afniq n Ccix Lmuhub). *J. Cult. Herit.* **2021**, *49*, 289–297. [[CrossRef](#)]
3. Bonizzoni, L.; Caglio, S.; Frezzato, F.; Martini, M.; Villa, V.; Galli, A. Balla's Bouquet: A Pigment Study for Flowers and Lights. *J. Cult. Herit.* **2021**, *52*, 164–170. [[CrossRef](#)]
4. Bonizzoni, L.; Bruni, S.; Galli, A.; Gargano, M.; Guglielmi, V.; Ludwig, N.; Lodi, L.; Martini, M. Non-Invasive in Situ Analytical Techniques Working in Synergy: The Application on Graduals Held in the Certosa Di Pavia. *Microchem. J.* **2016**, *126*, 172–180. [[CrossRef](#)]
5. Bonizzoni, L.; Bruni, S.; Gargano, M.; Guglielmi, V.; Zaffino, C.; Pezzotta, A.; Pilato, A.; Auricchio, T.; Delvaux, L.; Ludwig, N. Use of Integrated Non-Invasive Analyses for Pigment Characterization and Indirect Dating of Old Restorations on One Egyptian Coffin of the XXI Dynasty. *Microchem. J.* **2018**, *138*, 122–131. [[CrossRef](#)]
6. Bracci, S.; Cantisani, E.; Conti, C.; Magrini, D.; Vettori, S.; Tomassini, P.; Marano, M. Enriching the Knowledge of Ostia Antica Painted Fragments: A Multi-Methodological Approach. *Spectrochim. Acta Part A Mol. Biomol. Spectrosc.* **2022**, *265*, 120260. [[CrossRef](#)]
7. Bracci, S.; Cagnini, A.; Colombini, M.P.; Cuzman, O.A.; Fratini, F.; Galeotti, M.; Magrini, D.; Manganelli del Fà, R.; Porcinai, S.; Rescic, S.; et al. A Multi-Analytical Approach to Monitor Three Outdoor Contemporary Artworks at the Gori Collection (Fattoria Di Celle, Santomato, Pistoia, Italy). *Microchem. J.* **2016**, *124*, 878–888. [[CrossRef](#)]
8. Bartolozzi, G.; Bracci, S.; Cantisani, E.; Iannaccone, R.; Magrini, D.; Picollo, M. Non-Invasive Techniques Applied to the Alchemical Codex of the State Archive of Florence. *Spectrochim. Acta Part A Mol. Biomol. Spectrosc.* **2020**, *240*, 118562. [[CrossRef](#)]
9. Pinna, D.; Bracci, S.; Magrini, D.; Salvadori, B.; Andreotti, A.; Colombini, M.P. Deterioration and Discoloration of Historical Protective Treatments on Marble. *Environ. Sci. Pollut. Res.* **2022**, *29*, 20694–20710. [[CrossRef](#)]

10. Titubante, M.; Marconi, C.; Citiulo, L.; Mosca Conte, A.; Mazzuca, C.; Petrucci, F.; Pulci, O.; Tumiate, M.; Wang, S.; Micheli, L.; et al. Analysis and Diagnosis of the State of Conservation and Restoration of Paper-Based Artifacts: A Non-Invasive Approach. *J. Cult. Herit.* **2022**, *55*, 290–299. [[CrossRef](#)]
11. Macro, N.; Ioele, M.; Cattaneo, B.; De Cesare, G.; Di Lorenzo, F.; Storari, M.; Lazzari, M. Detection of Bronze Paint Degradation Products in a Contemporary Artwork by Combined Non-Invasive and Micro-Destructive Approach. *Microchem. J.* **2020**, *159*, 105482. [[CrossRef](#)]
12. Casanova, E.; Pelé-Meziani, C.; Guilminot, É.; Mevellec, J.-Y.; Riquier-Bouquet, C.; Vinçotte, A.; Lemoine, G. The Use of Vibrational Spectroscopy Techniques as a Tool for the Discrimination and Identification of the Natural and Synthetic Organic Compounds Used in Conservation. *Anal. Methods* **2016**, *8*, 8514–8527. [[CrossRef](#)]
13. Doménech-Carbó, M.T.; Doménech-Carbó, A.; Gimeno-Adelantado, J.V.; Bosch-Reig, F. Identification of Synthetic Resins Used in Works of Art by Fourier Transform Infrared Spectroscopy. *Appl. Spectrosc.* **2001**, *55*, 1590–1602. [[CrossRef](#)]
14. Rosi, F.; Daveri, A.; Moretti, P.; Brunetti, B.G.; Miliiani, C. Interpretation of Mid and Near-Infrared Reflection Properties of Synthetic Polymer Paints for the Non-Invasive Assessment of Binding Media in Twentieth-Century Pictorial Artworks. *Microchem. J.* **2016**, *124*, 898–908. [[CrossRef](#)]
15. Ludwig, N.; Orsilli, J.; Bonizzoni, L.; Gargano, M. UV-IR Image Enhancement for Mapping Restorations Applied on an Egyptian Coffin of the XXI Dynasty. *Archaeol. Anthropol. Sci.* **2019**, *11*, 6841–6850. [[CrossRef](#)]
16. Mannetti, T.R.; Chelli, N.; Vecchioli, G. *Saturnino Gatti nella Chiesa di San Panfilo a Tornimparte*; Ferri, A., Ed.; Edizioni del Gallo Cedrone: L'Aquila, Italy, 1992.
17. Bonizzoni, L.; Caglio, S.; Galli, A.; Lanteri, L.; Pelosi, C. Materials and technique: The first look at Saturnino Gatti. *Appl. Sci.* **2023**, submitted.
18. Mercurio, M.; Rossi, M.; Izzo, F.; Cappelletti, P.; Germinario, C.; Grifa, C.; Petrelli, M.; Vergara, A.; Langella, A. The Characterization of Natural Gemstones Using Non-Invasive FT-IR Spectroscopy: New Data on Tourmalines. *Talanta* **2018**, *178*, 147–159. [[CrossRef](#)]
19. Bonizzoni, L.; Caglio, S.; Galli, A.; Poldi, G. Comparison of three portable EDXRF spectrometers for pigment characterization. *X-Ray Spectrom.* **2010**, *39*, 233–242. [[CrossRef](#)]
20. Germinario, C.; Francesco, I.; Mercurio, M.; Langella, A.; Sali, D.; Kakoulli, I.; De Bonis, A.; Grifa, C. Multi-Analytical and Non-Invasive Characterization of the Polychromy of Wall Paintings at the Domus of Octavius Quartio in Pompeii. *Eur. Phys. J. Plus* **2018**, *133*, 359. [[CrossRef](#)]
21. Briani, F.; Caridi, F.; Ferella, F.; Gueli, A.M.; Marchegiani, F.; Nisi, S.; Paladini, G.; Pecchioni, E.; Politi, G.; Santo, A.P.; et al. Multi-technique characterization of painting drawings of the pictorial cycle at the San Panfilo Church in Tornimparte (AQ). *Appl. Sci.* **2023**, *13*, 6492. [[CrossRef](#)]
22. Izzo, F.; Germinario, C.; Grifa, C.; Langella, A.; Mercurio, M. External Reflectance FTIR Dataset (4000–400 cm^{-1}) for the Identification of Relevant Mineralogical Phases Forming Cultural Heritage Materials. *Infrared Phys. Technol.* **2020**, *106*, 103266. [[CrossRef](#)]
23. Invernizzi, C.; Rovetta, T.; Licchelli, M.; Malagodi, M. Mid and Near-Infrared Reflection Spectral Database of Natural Organic Materials in the Cultural Heritage Field. *Int. J. Anal. Chem.* **2018**, *2018*, 1–16. [[CrossRef](#)]
24. Mazzinghi, A. XRF analyses for the study of painting technique and degradation on frescoes by Beato Angelico: First results. *Il Nuovo Cim.* **2014**, *37*, 253–262. [[CrossRef](#)]
25. Gutman Levstik, M.; Mladenovič, A.; Kriznar, A.; Dolenc, S. A Raman microspectroscopy-based comparison of pigments applied in two gothic wall paintings in Slovenia. *Period. Mineral.* **2019**, *88*, 95–104. [[CrossRef](#)]
26. Miliiani, C.; Rosi, F.; Daveri, A.; Brunetti, B.G. Reflection Infrared Spectroscopy for the Non-Invasive in Situ Study of Artists' Pigments. *Appl. Phys. A* **2012**, *106*, 295–307. [[CrossRef](#)]
27. Kahrim, K.; Daveri, A.; Rocchi, P.; de Cesare, G.; Cartechini, L.; Miliiani, C.; Brunetti, B.G.; Sgamellotti, A. The Application of in Situ Mid-FTIR Fibre-Optic Reflectance Spectroscopy and GC-MS Analysis to Monitor and Evaluate Painting Cleaning. *Spectrochim. Acta Part A Mol. Biomol. Spectrosc.* **2009**, *74*, 1182–1188. [[CrossRef](#)] [[PubMed](#)]
28. Rampazzi, L.; Brunello, V.; Corti, C.; Lissoni, E. Non-Invasive Techniques for Revealing the Palette of the Romantic Painter Francesco Hayez. *Spectrochim. Acta Part A Mol. Biomol. Spectrosc.* **2017**, *176*, 142–154. [[CrossRef](#)] [[PubMed](#)]
29. Scremin, B.F. Raman Study of a Work of Art Fragment. *Vib. Spectrosc.* **2018**, *99*, 162–166. [[CrossRef](#)]
30. Armetta, F.; Giuffrida, D.; Ponterio, R.C.; Falcon Martinez, M.F.; Briani, F.; Pecchioni, E.; Alba Patrizia Santo, A.P.; Ciaramitaro, V.C.; Saladino, M.L. Looking for the original materials and evidence of restoration at the Vault of the San Panfilo Church in Tornimparte (AQ). *Appl. Sci.* **2023**, to be submitted.
31. Vagnini, M.; Miliiani, C.; Cartechini, L.; Rocchi, P.; Brunetti, B.G.; Sgamellotti, A. FT-NIR Spectroscopy for Non-Invasive Identification of Natural Polymers and Resins in Easel Paintings. *Anal. Bioanal. Chem.* **2009**, *395*, 2107–2118. [[CrossRef](#)]
32. Alberghina, M.F.; Germinario, C.; Bartolozzi, G.; Bracci, S.; Grifa, C.; Izzo, F.; Russa, M.F.L.; Magrini, D.; Massa, E.; Mercurio, M.; et al. The Tomb of the Diver and the Frescoed Tombs in Paestum (Southern Italy): New Insights from a Comparative Archaeometric Study. *PLoS ONE* **2020**, *15*, e0232375. [[CrossRef](#)] [[PubMed](#)]
33. Cultrone, G.; Arizzi, A.; Sebastián, E.; Rodríguez-Navarro, C. Sulfation of Calcitic and Dolomitic Lime Mortars in the Presence of Diesel Particulate Matter. *Environ. Geol.* **2008**, *56*, 741–752. [[CrossRef](#)]

34. Lanteri, L.; Calandra, S.; Briani, F.; Germinario, C.; Izzo, F.; Pagano, S.; Pelosi, C.; Santo, A.P. 3D Photogrammetric Survey, Raking Light Photography and Mapping of Degradation Phenomena of the Early Renaissance Wall Paintings by Saturnino Gatti—Case Study of the St. Panfilo Church in Tornimparte (L'Aquila, Italy). *Appl. Sci.* **2023**, *13*, 5689. [[CrossRef](#)]
35. Germinario, L.; Giannossa, L.C.; Lezzerini, M.; Mangone, A.; Mazzoli, C.; Pagnotta, S.; Spampinato, M.; Zoleo, A.; Eramo, G. Petrographic and chemical characterization of the frescoes by Saturnino Gatti (central Italy, 15th century): Microstratigraphic analyses on thin sections. *Appl. Sci.* **2023**. *to be submitted*.
36. Comite, V.; Bergomi, A.; Lombardi, C.A.; Fermo, P. Characterization of soluble salts on the frescoes by Saturnino Gatti in the church of San Panfilo in Villagrande di Tornim-partre (L'Aquila). *Appl. Sci.* **2023**. *to be submitted*.

Disclaimer/Publisher's Note: The statements, opinions and data contained in all publications are solely those of the individual author(s) and contributor(s) and not of MDPI and/or the editor(s). MDPI and/or the editor(s) disclaim responsibility for any injury to people or property resulting from any ideas, methods, instructions or products referred to in the content.